Title

Blockade of Kv1.3 channels ameliorates radiation-induced brain injury.

Permalink

https://escholarship.org/uc/item/92x958tb

Journal

Neuro-Oncology, 16(4)

Authors

Peng, Ying

Lu, Kui

Li, Zichen

et al.

Publication Date

2014-04-01

DOI

10.1093/neuonc/not221

Peer reviewed

Neuro-Oncology

Blockade of Kv1.3 channels ameliorates radiation-induced brain injury

Ying Peng[†], Kui Lu[†], Zichen Li, Yaodong Zhao, Yiping Wang, Bin Hu, Pengfei Xu, Xiaolei Shi, Bin Zhou, Michael Pennington, K. George Chandy, and Yamei Tang

Department of Neurology, Sun Yat-sen Memorial Hospital, Sun Yat-sen University, Guangzhou, China (Y.P., K.L., Z.L., Y.W., B.H., P.X., X.S., Y.T.); Department of Neurosurgery, Shanghai 10th People's Hospital, Tongji University, Shanghai, China (Y.Z., B.Z.); Peptides International, Louisville, Kentucky (M.P.); Department of Physiology and Biophysics, University of California, Irvine, Irvine, California (K.G.C.)

Corresponding author: Yamei Tang, PhD, Department of Neurology, Sun Yat-sen Memorial Hospital, Sun Yat-sen University, No. 107, Yan Jiang Xi Rd, Guangzhou, Guangdong Province, China, 510120 (yameitang@hotmail.com).
[†]These authors contributed equally to this work.

Background. Tumors affecting the head, neck, and brain account for significant morbidity and mortality. The curative efficacy of radiotherapy for these tumors is well established, but radiation carries a significant risk of neurologic injury. So far, neuroprotective therapies for radiation-induced brain injury are still limited. In this study we demonstrate that Stichodactyla helianthus (ShK)–170, a specific inhibitor of the voltage-gated potassium (Kv)1.3 channel, protected mice from radiation-induced brain injury.

Methods. Mice were treated with ShK-170 for 3 days immediately after brain irradiation. Radiation-induced brain injury was assessed by MRI scans and a Morris water maze. Pathophysiological change of the brain was measured by immunofluorescence. Gene and protein expressions of Kv1.3 and inflammatory factors were measured by quantitative real-time PCR, reverse transcription PCR, ELISA assay, and western blot analyses. Kv currents were recorded in the whole-cell configuration of the patch-clamp technique.

Results. Radiation increased Kv1.3 mRNA and protein expression in microglia. Genetic silencing of Kv1.3 by specific short interference RNAs or pharmacological blockade with ShK-170 suppressed radiation-induced production of the proinflammatory factors interleukin-6, cyclooxygenase-2, and tumor necrosis factor–α by microglia. ShK-170 also inhibited neurotoxicity mediated by radiation-activated microglia and promoted neurogenesis by increasing the proliferation of neural progenitor cells.

Conclusions. The therapeutic effect of ShK-170 is mediated by suppression of microglial activation and microglia-mediated neurotoxicity and enhanced neurorestoration by promoting proliferation of neural progenitor cells.

Keywords: Kv1.3, microglia, radiation, ShK.

Tumors affecting the head, neck, and brain account for significant morbidity and mortality, with an incidence of 6.5–12.5 per 100 000 in the United States[1,2] and a higher incidence in southeastern Asia, where incidence of nasopharyngeal carcinoma for males is 6.5% and for females 2.8%.[3] Radiation is an important adjuvant therapy for these types of tumors, and its curative efficacy is well established. However, therapeutic irradiation carries the risk of neurologic injury including focal cerebral necrosis, neurocognitive deficits, cerebrovascular disease, myelopathy, and brachial plexopathy.[4,5] Although the acetylcholinesterase inhibitor donepezil has been reported to improve cognitive function in irradiated brain tumor patients, neuroprotective therapies for radiation-induced brain injury are still limited.[6]

Radiation to the brain induces a profound inflammatory response.[7] Local inflammation is a major contributor to white matter damage and cerebral edema.[8,9] Within a few hours of radiation, microglia get activated, change their shape from "ramified" to "amoeboid," activate transcription factors (eg, nuclear factor-kappaB), and produce proinflammatory mediators (eg, tumor necrosis factor [TNF]–α, interleukin [IL]-1 and -6, and cyclooxygenase [Cox]-2) that impair neurogenesis[10,11] and contribute to CNS injury.[12–15] Radiation has also been reported to deplete neural progenitor cells (NPCs) from the subgranular zone (SGZ) of the hippocampal dentate gyrus and suppress neurogenesis.[16–18] Therefore, suppressing the destructive inflammatory response and promoting neurogenesis might limit radiation-induced brain injury.

The voltage-gated Kv1.3 potassium channel plays an important role in cell types—microglia, T cells, dendritic cells, and NPCs—likely to participate in radiation-induced CNS injury. Kv1.3 is upregulated during microglial activation,[19,20] and microglia-mediated damage to neurons requires Kv1.3 channel activity.[21] Kv1.3 expression is

increased during the activation of effector-memory T cells, and pharmacological blockade of Kv1.3 in these cells suppresses proliferation, cytokine production, and in vivo migration and ameliorates experimental autoimmune encephalomyelitis.[22] Kv1.3 blockade of dendritic cells in the CNS impairs upregulation of CD83, CD80, CD86, CD40, and IL-12.[23] Kv1.3 is present in NPCs. Blockade of this channel enhances proliferation of these cells[24] and protects them from the toxic effects of the T-cell mediator Grb2.[25] Targeting Kv1.3 channels with a selective blocker might therefore reduce radiation-induced brain injury by targeting the key cells involved in the inflammatory process (microglia, lymphocytes, dendritic cells), while promoting neurogenesis. For these studies we chose Stichodactyla helianthus (ShK)–170, a selective peptide inhibitor of Kv1.3 with picomolar potency, because it is effective in rodent experimental autoimmune encephalomyelitis and has durable pharmacological activity[26] and an excellent safety profile in rodents.[26] Here, we demonstrate that ShK-170 ameliorates radiation-induced brain injury by suppressing microglial activation and the production of proinflammatory factors and by promoting neurorestoration.

Materials and Methods

Cultures of Primary Microglia and BV2 Microglia

Primary microglia cultures derived from newborn mice were prepared from mixed glia cultures with the "shaking off" method as described previously.[27] The immortalized murine microglia BV2 cell line that exhibits phenotypic and functional properties of reactive microglial cells was obtained from the Cell Center of Peking Union Medical College and cultured as described.[28] The BV2 cell line is useful for in vitro studies of microglia activation,[28] and our supplementary materials show that biological responses of primary microglia and BV2 to radiation are similar.

Cell Irradiation and Treatment

We tested the radiation effect with doses of 3, 5, 8, and 10 Gy. Inflammatory mediators did not change at 3 or 5 Gy but increased significantly at 8 and 10 Gy. Since earlier studies had reported that 10 Gy was the optimal radiation dose to activate microglia,[9] we used this dose for our studies. Primary microglia and BV2 microglia were divided into 3 groups: unirradiated controls, irradiated controls, and irradiated with ShK-170 pretreatment. ShK-170 was added at 0.1, 1, 10, and 100 nM for 1 h before irradiation. Cells were then irradiated using a 6-megavolt β-ionizing-ray linear accelerator (Siemens). Cells or culture supernatants were collected at 4 h, 12 h, 1 d, and 2 d post-irradiation.

Animal Irradiation and Treatment

Adult 6- to 8-week-old male Balb/c mice weighing 20–25 g were used in this study. All procedures followed the guideline of the Chinese National Institute of Health for humane care, and protocols were approved by the committee on animal research at Sun Yat-sen University. Mice were randomly divided into the following groups: unirradiated controls, irradiated mice administered saline (placebo controls), and irradiated mice administered ShK-170. For irradiation, animals were anesthetized with 10% chloral hydrate (600 mg/kg) administered by intraperitoneal injection. Irradiation was administered using the Siemens 6-megavolt β-ionizing-ray linear accelerator as previously described.[29] The head of each mouse was placed in a treatment field (2×2 cm^2) within the confines of the whole brain from the post-canthus line to the post-aurem line. A single dose of 30 Gy was given at a rate of 3 Gy/min and a source-to-skin distance of 100 cm. For the treatment protocols, mice were administrated saline or ShK-170

(100 μg/kg/d) once daily by i.p. injection. The controls received anesthetic procedures at the same time as those irradiated. Mice were sacrificed at 4 time points: 4 h, 1 d, 3 d, and 14 d post-irradiation or were followed for 8 weeks to evaluate spatial learning activity and 16 weeks to detect long-standing brain atrophy by MRI scans. The brains of 5 mice in each group were used for morphological examination on the third day post-irradiation, while 4 were used for western blotting and real-time PCR. For detection of neurogenesis in the dentate gyrus, bromodeoxyuridine (BrdU; Sigma) at 100 mg/kg i.p. was administered starting 7 days before animals were sacrificed, once daily for 6 consecutive days, and finally 3 times (10 h, 6 h, and 2 h) prior to sacrifice.[30]

MRI Scanning

MRI scans were performed at 16 weeks ($n = 6$ for each group) post-irradiation by a 3T nuclear magnetic resonance scanner (Intera, Philips Medical Systems) and a 5-cm linearly polarized birdcage radiofrequency animal coil (Chenguang Medical Technologies). Mice were anesthetized and prostrated on a custom-made holder with strapping to minimize head motion while respiration was monitored. Coronal and transverse T2-weighted MRIs were obtained using a 2-dimensional turbo spin echo sequence (repetition time/echo time, 1600 ms/125 ms; flip angle, 90°; field of view, 40 mm; matrix, 200/400 r, echo planar imaging factor, 1; turbo spin echo factor, 10; number of signal averages, 14; slice thickness, 2 mm; intersection gap, −0.9 mm; total scan time, 11 min). The transverse slices were paralleled with the brainstem and ranged from the superior of the parietal lobe to the inferior of the temporal lobe. Coronal slices were obtained on the vertical orientation to the transverse slice and ranged from the frontal to the posterior edges of the cerebrum. The final numbers of MRIs were coronal = 6, transverse = 5. Since irradiated animals showed significant enlargement of lateral ventricles, the size of the ventricles was compared between groups. The frontal and occipital horn ratio is a measure of the volume of the lateral ventricle.[31] This ratio was calculated as the sum of the maximal width of the frontal horn and occipital horn of the lateral ventricles divided by the maximum brain width taken in an axial slice at the level of the cerebral aqueduct. An enlarged lateral ventricle indicates cerebral cortex atrophy.[32]

Morris Water Maze

Spatial learning and memory were evaluated in animals 8 weeks post-irradiation using the Morris water maze.[33] Mice were trained in the Morris water maze for 6 days with 4 trials per day ($n = 7$ for each group). In each trial the animal was released into the water and was given 1 min to find the hidden platform. When the animal found the platform within 1 min, it was given a further 15 s to stay on the platform. If it did not find the platform within 1 min, it was guided to the platform and then allowed to stay on the platform for a further 15 s. Latency in finding the platform and swim path length were analyzed by a computerized video tracking system (DMS-2). The average latency and length of swim of 6 consecutive days' trials were used in this study. The probe trial was performed on day 5, when the mice were allowed 60 s to explore the water maze platform with the platform removed. The time spent in each quadrant and platform location crossings were recorded for the 60 s probe trial semiautomatically by DMS-2. After the maze test, the animal was dried with a towel and brought back to its cage beside an electric radiator.

Electrophysiology

Unstimulated, radiated, or trypsinized lipopolysaccharide-stimulated primary microglia were plated onto poly-L-lysine coated glass coverslips and allowed to attach for 20 min at 37°C. Kv currents were then recorded at room temperature in the whole-cell configuration of the patch-clamp technique using an EPC-10 amplifier (HEKA). The external solution

contained (mM) 160 NaCl, 4.5 KCl, 2 CaCl$_2$, 1 MgCl$_2$, and 10 HEPES (4-(2-hydroxyethyl)-1-piperazine ethanesulfonic acid), pH 7.4, osmolality 300 mmol/kg. The internal pipette solution contained (mM) 160 KF, 2 MgCl$_2$, 10 HEPES, and 10 EGTA (ethylene glycol tetraacetic acid), pH 7.2, osmolality 300 mmol/kg. Pipette resistances were 1.5–3 megaohms. The holding potential was −80 mV. Current traces were exported into IGOR Pro software for figure assembly. The Kv current in microglia were determined to be Kv1.3 based on their cumulative inactivation, a characteristic of Kv1.3, and their sensitivity to ShK-170 at picomolar concentrations.

Coculture of Primary Mice Neurons and Primary Microglia

Primary cultures of mice hippocampal neurons were obtained from postnatal day 0 embryonic mouse brains as described[34] and were cocultured with primary microglia indirectly in 24-well-plate chambers (pore size 0.4 µm; BD Falcon) to study the effect of radiation-activated microglia on the survival of neuronal cells. In this coculture system, microglial cells communicate with primary mice neuronal cells through the semipermeable membrane, avoiding direct contact.

Inhibiting Expression of Kv1.3 by RNA Short Interference

The short interference (si)RNA sequences used for silencing of mouse Kv1.3 were chemically synthesized by GenePharma: forward and reverse RNA strands were: sense, CCAUGACAACUGUUGGUUATT; antisense, UAACCAACA GUUGUCAUGGTT. Control nonspecific sequences were: sense, UUCUCCG AACGUGUCACGUTT; antisense, ACGUGACACGUUCGGAGAATT. The medium was exchanged for Opti-MEM minimal essential medium (Invitrogen) before RNA interference transfection. Briefly, 5 µL of Lipo2000 (transfectamine solution; Invitrogen) and 5 µL siRNA were gently mixed with Opti-MEM to a final volume of 500 µL and incubated at room temperature for 30 min. Then the transfection agent/siRNA complex was added dropwise onto the cells (25 nM final concentration), which were incubated for 6 h at 37°C until a medium change with 1% fetal bovine serum–Dulbecco's modified Eagle's medium with F12. Then cells were irradiated as previously here described. The cells and the supernatant were collected at 12 h and 1 d postirradiation.

Immunohistochemistry and Immunocytochemistry

For morphological examination in vivo, mice were anesthetized, followed by intracardiac perfusion with normal saline and 4% paraformaldehyde (PFA) in sequence. Afterward, the brains of each group and the spleens of the irradiated group were removed, postfixed in 4% PFA overnight, and dehydrated in a sucrose gradient. Serial sections with thickness of 10 µm or 30 µm were cut on a sliding knife with a cryostat microtome. Sections were blocked in a solution containing 5% normal goat serum for 1 h after rinsing in 0.3% Triton X-100 for 30 min at room temperature. Then the sections were incubated at 4°C overnight with primary antibodies against Iba1 (1:250; Wako Pure Chemicals), Kv1.3 (1:50; NeuroMab), β-tubulin class III (1:400; Epitomics), CD3 (1:100; R&D Systems), CD20 (1:50; OriGene Technologies), and CD68 (1:200; Abcam). After washing, the sections were stained with fluorescent-conjugated secondary antibody including goat anti-mouse Alexa-488 (Jackson ImmunoResearch), goat anti-rat Alexa-594 (Jackson ImmunoResearch), or donkey anti-rabbit Cy3 (1:200; Millipore) for 100 min at room temperature. After nuclear staining with 4′,6′-diamidino-2-phenylindole for 10 min, sections were coverslipped with glycerol, and fluorescent images were obtained with a fluorescence microscope (Olympus). For double-staining of BrdU and Neuronal Nuclei (NeuN), sections with a thickness of 30 µm were microwaved for heat-induced epitope retrieval, incubated with 2 N HCl at 37°C for 30 min, and rinsed in 5% normal goat serum and 0.3% Triton X-100 sequentially as described previously. The following primary antibodies were used overnight at 4°C: rat anti-BrdU (1:300; AbD Serotec) and monoclonal mouse anti-NeuN

(1:100; Millipore). Afterward, primary antibodies were detected with either Alexa-488– or Alexa-594–conjugated secondary antibodies (1:300; Jackson ImmunoResearch). Immnohistochemical avidin-biotin complex kits (Zhongshan Goldenbridge) were applied to investigate CD20 of brain and spleen, which was followed by diaminobenzidine and hematoxylin staining.

For in vitro fluorescence labeling, primary microglia or BV2 cells were seeded in 24-well plates and treated with 100 nM ShK-170. At 24 h postirradiation, cells were fixed in 4% PFA for 30 min. After blocking with 5% normal goat serum for 30 min, cells were incubated at 4°C overnight with primary antibodies against CD11b (1:50; Abcam) or Kv1.3 (1:50; Chemicon). After washing, cells were incubated for 1 h with appropriate fluorescent-conjugated secondary antibodies: goat anti-mouse Cy3 (1:60; Boshide) or goat anti-rabbit fluorescein isothiocyanate (1:60; Sigma) and coverslipped in anti-fluorescence-quenching reagent (Boshide). Fluorescent images were obtained and analyzed as mentioned previously.

The percentage of microglial cells that were activated was determined for each group. CD11b$^+$, Iba1$^+$ (total microglia), and CD68$^+$ cells were counted in 5 random 200× fields for each repeated experiment. Resting microglia exhibited a branchlike form, while activated microglial cells were characterized by bigger soma and a round and amoeba-like shape.

In the study of neurogenesis, NeuN/BrdU-positive cells were counted and included in statistics if they were in the SGZ. Five sections per animal (6 mice in total) were counted.

Reverse Transcription PCR

Tissue and cells of various groups were lysed in 1 mL Trizol reagent (Invitrogen). Total RNA was harvested as described by the manufacturer's protocol and stored at −80°C until samples from all time points were collected for reverse transcription PCR. Total RNA (1 ug) was used for reverse transcription PCR using random hexamers and superscript reverse transcriptase II (TaKaRa) in a total volume of 20 µL. Reactions were performed according to the manufacturer's protocol. The cDNA was then used for PCR of murine inflammatory factor genes using gene-specific primers. PCR products were separated by electrophoresis through 2% agarose in Tris/borate/EDTA solution and imaged using a bio-gel imaging system (Genetics). Band intensities were determined using a gel imaging analysis system (Genetics).

Quantitative Real-time PCR

Total RNA from primary microglia and BV2 cells was extracted and reverse transcribed into cDNA using the protocols described here previously. Quantitative PCR in a final 20-µL reaction volume was performed using 50 ng of cDNA of each sample in a 96-well-plate format on a Roche 480 LightCycler Detection System. To allow standardization of the amount of cDNA added to each PCR reaction and to minimize the effects of individual difference on the results, quantitative PCR for the housekeeping gene *GAPDH* (glyceraldehyde 3-phosphate dehydrogenase) was performed for each sample. We used real-time PCR to simultaneously detect and quantify Cox-2, TNF-α, IL-6, and Kv1.3. The increase in the fluorescent signal was registered during the extension step of the reaction, and the data were analyzed by LightCycler 480 software 1.5 (Roche).

Immunoblotting

Total protein extracts were prepared and quantified from primary microglia, BV2 cells, or mouse brain. Kv1.3 expression after radiation and the effects of Kv1.3 siRNA and ShK-170 on radiation-induced Cox-2 expression in microglia were evaluated by western blot analysis. In brief, 40 µg of total proteins for each lane were separated by sodium dodecyl sulfate polyacrylamide gel electrophoresis and transferred onto a polyvinylidene difluoride membrane (Millipore) using an electrophoretic transfer apparatus (Bio-Rad). The

membrane was blocked with 5% bovine serum albumin in Tris-buffered saline + 0.05% Tween 20 (TBST) solution. The blots were laid on a shaker and incubated with polyclonal rabbit anti–Cox-2 (Cell Signaling Technology) and anti-Kv1.3 (Chemicon) in blocking solution overnight at 4°C. After washing with TBST, the membranes were probed with secondary antibodies by a goat anti-rabbit IgG horseradish peroxidase conjugate (Cell Signaling Technology) and the blots developed by enhanced chemiluminescence detection (Beyotime) by exposure to X-ray film. The relative densities of bands were analyzed with gel imaging analysis (Genetics).

Enzyme-linked Immunosorbent Assay

ELISAs were performed to measure levels of TNF-α, Cox-2, and IL-6 on the culture supernatants according to the manufacturer's instructions (Dakewei). Aliquots were stored at −80°C until ELISA was performed. The plate was read at 595 nm with a microplate reader, and data were analyzed with SoftMax Pro software.

Statistical Analysis

All data are presented as the mean of each treatment group ± SEM, and statistical analyses were performed using SPSS 17.0. For experiments that required immunostaining, the total immunolabeled cells were counted in 5 predetermined fields per coverslip or slide using a fluorescence microscope with a 10× or 40× objective. Three coverslips/slides were counted in each group. At least 3 independent experiments were performed. Differences were tested using either a 1-way ANOVA followed by Bonferroni's test for multiple comparisons or Student's t-test for 2-group comparisons. Two-tailed values of $P < .05$ were considered significant.

Results

Short-term treatment with ShK-170, a selective peptide inhibitor of Kv1.3 channels, reduces long-standing radiation-induced brain injury.

In previous reports, a single dose of 25 Gy radiation was used to induce brain injury in rats[35] or was used as hemisphere radiation on mice,[36] but the level of the microglial-derived proinflammatory factors did not increase with this dose.[14] We therefore used a single 30 Gy radiation dose to the head. We evaluated the effectiveness of ShK-170 in preventing brain damage in irradiated mice. For the treatment protocols, mice were administered saline or ShK-170 (100 μg/kg/d) once daily by i.p. injection for 3 consecutive days, starting 60 min before irradiation. At the 16th week post-irradiation, we determined the volume of the lateral ventricle in T2-weighted MRIs by measuring the frontal and occipital horn ratio; the higher the ratio, the larger the lateral ventricle. Radiated placebo-control mice (Rad group) showed significantly enlarged lateral ventricles compared with unirradiated control mice (control group) (Fig. 1A–C, $n = 6$ per group; $P < .05$), most likely reflecting atrophy of the cerebral cortex. Three days of ShK-170 therapy (100 μg/kg i.p. injection once daily), started immediately after radiation (ShK group), prevented the enlargement of the lateral ventricles (Fig. 1A–C; $n = 6$ per group, $P < .05$, ShK-170 vs Rad).

To evaluate the effect of ShK-170 on the impairment of neurologic deficits after brain irradiation, we used the Morris water maze at 8 weeks post-irradiation to assess spatial learning and memory. The time (latency) and the path length to find a hidden platform (northwest quadrant of the water maze) was longest in irradiated placebo-control mice (Fig. 2A and B). Irradiated mice treated with
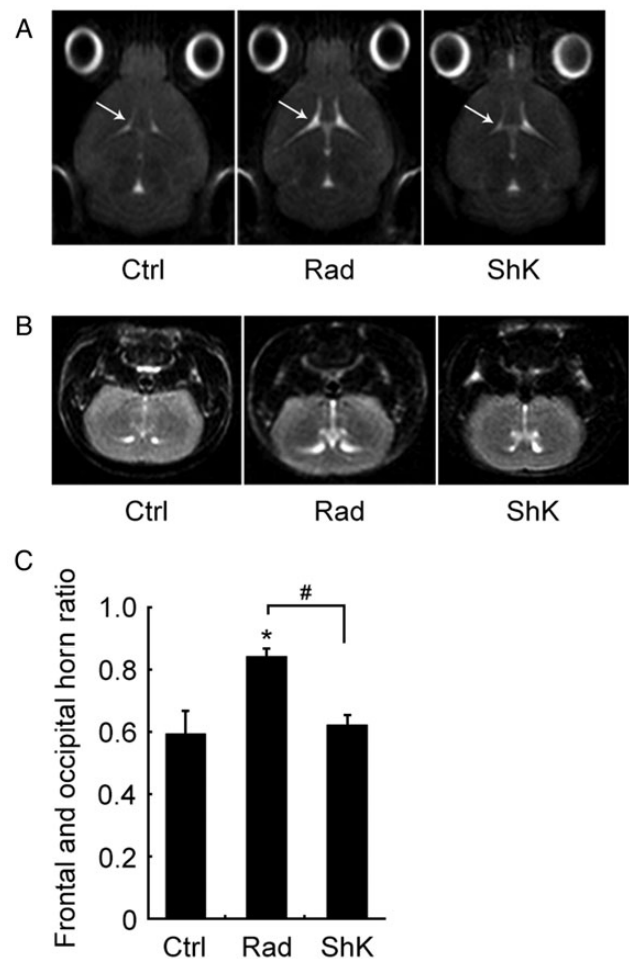

Fig. 1. MRI scan of mice brains shows enlargement of lateral ventricle after irradiation is alleviated by ShK-170. (A) Transverse scan. (B) Coronal scan. T2-weighted MRIs at week 16 post-irradiation display lateral ventricles (highlighted by white arrow) in different groups. Ctrl: unirradiated control mice ($n = 6$); Rad: radiated mice administered placebo for 3 days post-irradiation ($n = 6$); ShK: irradiated mice treated with ShK-170 (100 μg/kg/d) for 3 days following radiation ($n = 6$). Data are from 2 independent experiments. (C) Histogram showing the frontal to occipital horn ratio in the 3 groups of mice. Mean ± SEM; *$P < .01$ when irradiated group is compared with unirradiated control group; #$P < .05$ when ShK-170–treated group is compared with irradiated group; $n = 6$.

ShK-170 had significantly shorter latency and path length, but longer than unirradiated control mice (Fig. 2A and B). On day 5 of the study, irradiated ShK-170–treated mice spent significantly more time in the target (northwest) quadrant of the water maze (27.03% ± 2.11%) than irradiated placebo-control mice (22.61% ± 3.14%, $P < .05$), suggestive of improved spatial memory, but they spent less time in the target quadrant than unirradiated controls (34.97% ± 3.04%; Fig. 2C and D). ShK-170 likely enters the brain after radiation-mediated disruption of the blood–brain barrier.[37] Because the peptide maintains blood levels above the half-maximal inhibitory concentration value for Kv1.3 block for 3–5 days after a single injection,[38] Kv1.3-blocking concentrations of ShK-170 are likely to have been present for 8 days in treated mice (ie, 5 days after the third administration of ShK-170). Together, the data from
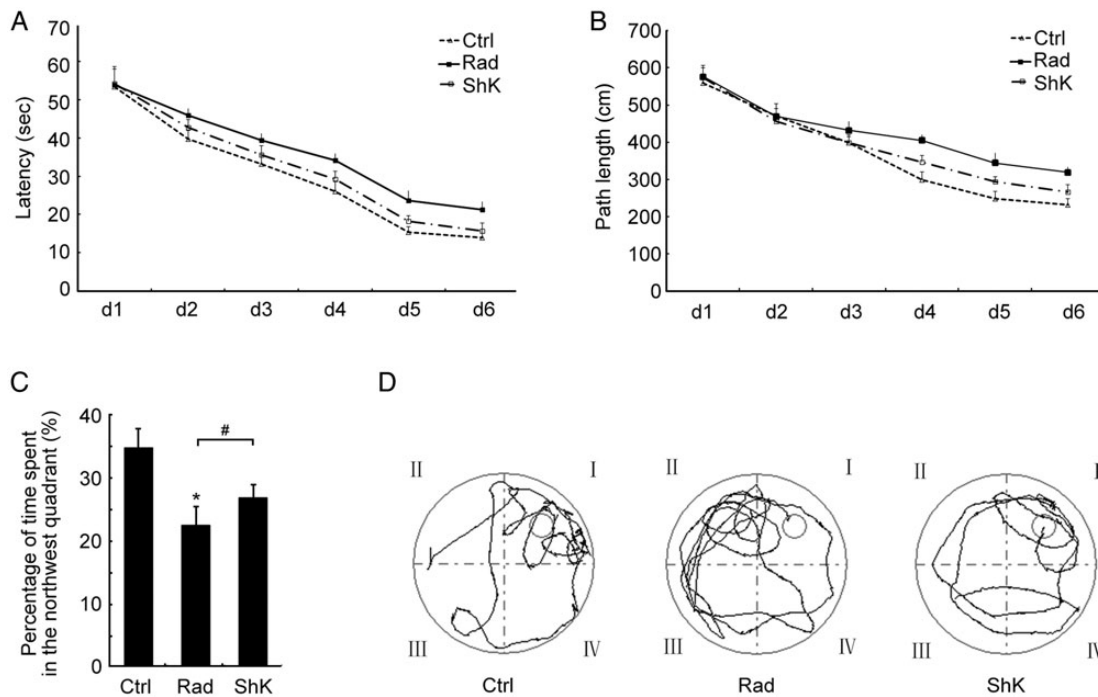
Fig. 2. ShK-170 improves spatial learning in mice after irradiation. (A) The latency and (B) swim path length before arrival on the platform were recorded for 6 consecutive days in each group. (C) Percentage of time in the northwest quadrant of the water maze for mice in each group. The difference between different groups was assessed using probe trials on day 5 of training and was analyzed using a 1-way ANOVA followed by Bonferroni's test. *$P < .01$ when irradiated group is compared with unirradiated control group; #$P < .05$ when ShK-170–treated group is compared with irradiated group; $n = 7$. (D) Swimming trail of each group in probe trial was recorded by DMS-2.

the MRI and Morris water maze suggest that ShK-170 therapy during the acute phase of radiation-induced brain injury can reduce long-standing radiation-induced brain injury. In the ensuing paragraphs, we present evidence to demonstrate that the therapeutic effect of ShK-170 is due to a combination of suppression of microglial function and neurorestoration via enhanced proliferation of NPCs.

Genetic Silencing or Pharmacological Blockade of Kv1.3 Suppresses Radiation-induced Production of Proinflammatory Mediators

A single dose of ionizing radiation (10 Gy) administered to freshly isolated mouse microglia or to mouse BV2 microglial cells (a useful model for in vitro studies of microglia)[28] induced a significant increase in Kv1.3 protein expression, which began 4 h after radiation and remained elevated for 2 days (Fig. 3A and B; Supplementary Fig. S1A–C). Patch-clamp experiments revealed increased-amplitude Kv currents in irradiated primary microglia (Fig. 3C and D), comparable to the ShK-170–sensitive Kv current seen in lipopolysaccharide-activated primary mouse microglia (Supplementary Fig. S1D and E). In vivo experiments confirmed the in vitro data. Balb/c mice administered a single radiation dose of 30 Gy to the skull showed increased Kv1.3 protein expression in microglia isolated from the brain 1–3 days after radiation (Fig. 3E and F), and immunostains revealed Kv1.3 expression in Iba1+ microglia in irradiated brain (Fig. 3G). Taken together, these data demonstrate that radiation, both in vitro and in vivo, stimulates Kv1.3 protein expression in activated microglia.

In parallel with the increase in Kv1.3, both primary mouse microglia (Fig. 4A–C) and BV2 microglia (Supplementary Fig. S2A–E) increased production of proinflammatory factors IL-6, TNF-α, and Cox-2 following irradiation (10 Gy) in vitro. The mRNA levels of IL-6, Cox-2 (Fig. 4D–F), and TNF-α (Supplementary Fig. S2F) were also significantly increased in the brains of irradiated mice. Since lymphocytes can also produce proinflammatory mediators, we performed immunostaining experiments to determine whether radiation caused CNS infiltration by lymphocytes. No T- or B-lymphocytes were detected in the brain following radiation (Supplementary Figs. S3 and S4). Our results suggest that radiation-stimulated microglial activation contributes to the increased production of proinflammatory factors in the CNS.

We used genetic silencing of Kv1.3 with a Kv1.3-specific siRNA and pharmacological blockade by ShK-170 to establish a link between Kv1.3 upregulation and the production of proinflammatory factors. Due to the close similarity in radiation-induced responses of primary mouse microglia and BV2 microglia, we used BV2 microglia for these experiments. The Kv1.3-specific siRNA suppressed Kv1.3 protein levels in transfected microglia (Fig. 5A and B) and inhibited radiation-induced increases in IL-6, Cox-2, and TNF-α mRNA and protein in microglia (Fig. 5C and D, Supplementary Fig. S5). Pharmacological blockade of Kv1.3 channels with ShK-170 also inhibited radiation-induced increases in Kv1.3, IL-6, and Cox-2 in a dose-dependent manner (Fig. 5E). Mice administered ShK-170 (100 μg/kg) by i.p. injection, once daily for 3 days starting from the day of irradiation (30 Gy to the head), exhibited significantly reduced mRNA levels of Cox-2 and IL-6 (Fig. 4D–F), but not TNF-α (Supplementary
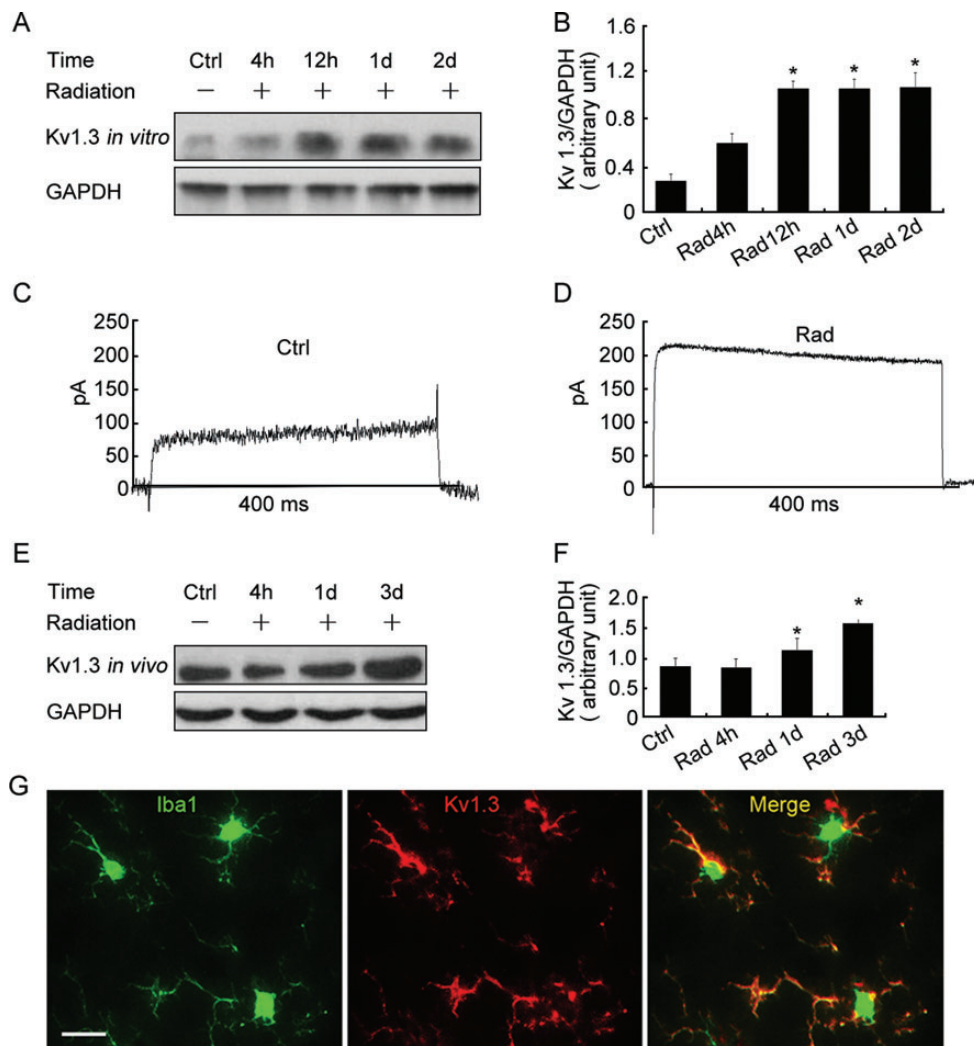
Fig. 3. Kv1.3 expression increases in microglia following irradiation. (A) Kv1.3 protein expression in primary mouse microglia determined by western blotting 4 h, 12 h, 1 d, and 2 d after radiation. (B) Densitometric analysis of western blot showing Kv1.3 vs glyceraldehyde 3-phosphate dehydrogenase (GAPDH). Mean ± SEM; $n = 3$; *$P < .05$ compared with unirradiated control group. (C and D) Kv currents in unirradiated and irradiated primary mouse microglia 12 h after radiation. (E) Kv1.3 protein expression in the brain of mice that received a single 30-Gy radiation dose to the head. (F) Densitometric analysis of western blot showing Kv1.3 vs GAPDH. Mean ± SEM; $n = 4$; *$P < .05$ compared with unirradiated control group. (G) Iba1 (a microglia/macrophage marker) and Kv1.3 colocalize in microglia in the brain of Balb/c mice that received a single dose of 30 Gy radiation to the head. Scale bar, 30 μm.

Fig. S2F). ShK-170 therapy also reduced expression of Iba1 in microglia and decreased the percentage of activated microglia immunostained by CD68 (Supplementary Fig. S6).

Kv1.3 Blockade Inhibits Microglia-mediated Neurotoxicity

We next explored whether the protective effect of ShK-170 was mediated, in part, by suppression of the neurotoxic effects of radiation-induced activated microglia and the proinflammatory factors they produced. We cocultured irradiated BV2 microglia and primary hippocampal neurons in a transwell system and irradiated microglial cells in the upper chamber and hippocampal neurons in the lower chamber. After coculture for 4 h or 12 h post-irradiation, apoptotic, neuronal cells were detected by double

staining with NeuN and terminal deoxynucleotidyl transferase deoxyuridine triphosphate nick end labeling (TUNEL), and the ratio of apoptotic to live neuronal cells was calculated. In a separate experiment, neuronal cells were pretreated with ShK-170 (10 nM or 100 nM) or medium for 1 h, then exposed to recombinant inflammatory factors (IL-6 and TNF-α). The ratio of apoptotic to live neuronal cells 12 h later was measured through NeuN and TUNEL staining.

Irradiated microglia induced greater apoptosis in neurons compared with unirradiated microglia ($P = .0001$ at 4 h, $P = .033$ at 12 h; Fig. 6A). Treatment of microglia with ShK-170 prior to radiation significantly reduced neurotoxicity ($P < .01$ at 4 h and 12 h; Fig. 6A). Residual ShK-170 is not the cause of this inhibition because irradiated microglial cells were washed 3 times before
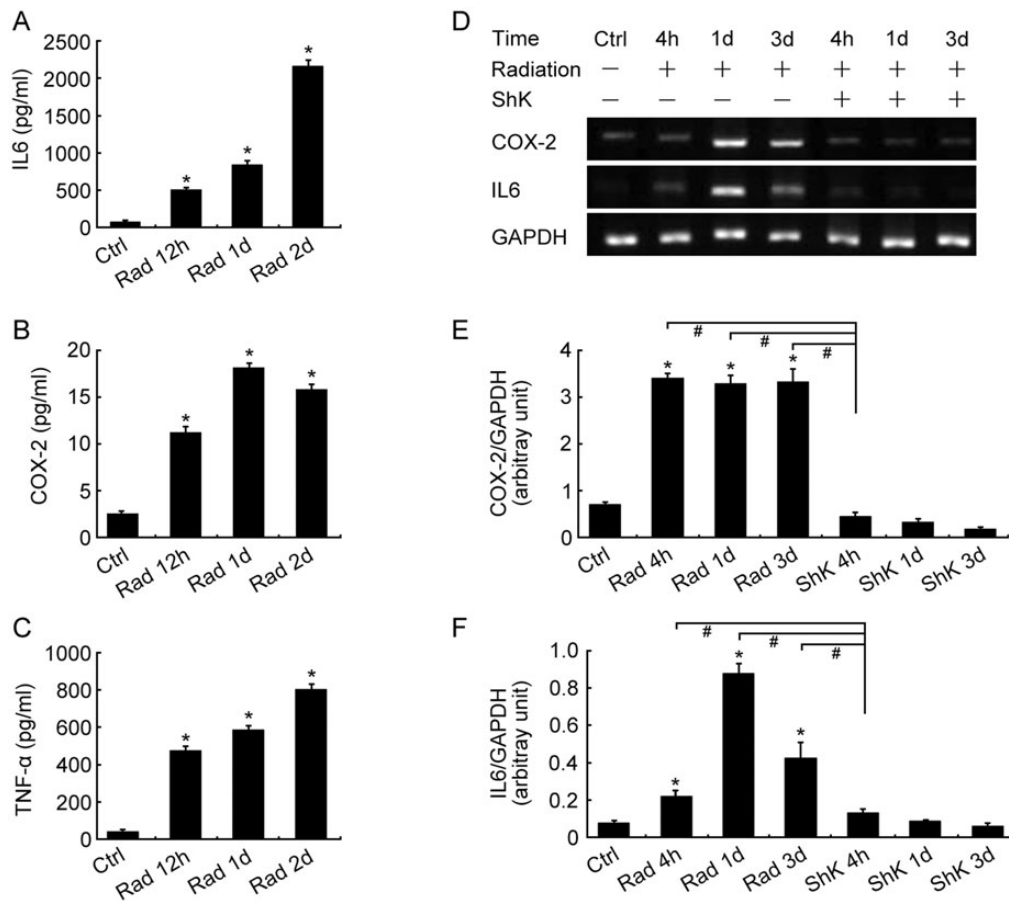
Fig. 4. Proinflammatory factors increase following irradiation. (A–C) IL-6, Cox-2, and TNF-α protein determined by ELISA in supernatants from cultured primary mouse microglia after a single dose of 10 Gy radiation. *$P < .05$, compared with unirradiated primary microglia controls. Data are obtained from 3 replicate wells. (D) A single 30 Gy dose of radiation to the head of Balb/c mice increased Cox-2 and IL-6 levels in the brain. Administration of ShK-170 (100 μg/kg/d) prevented radiation-induced increases in IL-6 and Cox-2 measured 4 h, 12 h, and 3 d after radiation. (E, F) Densitometric scans of the data in (D). Mean ± SEM; *$P < .01$ when irradiated group is compared with unirradiated group; #$P < .05$ when ShK-170–treated group is compared with irradiated group; $n = 4$ for each group at each time point.

initiating coculture. Furthermore, ShK-170 did not prevent neurotoxicity induced by recombinant IL-6 or TNF-α (Fig. 6B), indicating that it has no direct inhibitory effect on neurons and its inhibitory effect is directly on microglia. Thus, suppression of microglia-mediated neurotoxicity likely contributes to ShK-170's therapeutic effect in limiting brain injury due to radiation. The neurons stained with TUNEL and NeuN of these 3 groups are displayed in Fig. 6C.

ShK-170 Enhances Neurorestoration and Attenuates Radiation-induced Brain Injury

NPCs that contribute to the healing process following brain injury by promoting neurogenesis[39] are depleted 14 days after radiation-induced brain injury, and their differentiation into neurons is inhibited via microglia-mediated inflammatory mechanisms.[11,16,17,40] Since NPCs express Kv1.3, and blocking of this channel augments NPC proliferation,[24] we examined whether ShK-170 would promote neurogenesis following radiation. Mice that received a single dose of brain irradiation (30 Gy) had decreased numbers of neurons in the cortex (Fig. 7A and B) and hippocampus (Fig. 7C and D) identified by their decreased β-tubulin staining on day 3 post-irradiation ($P < .05$ in both cases; radiated placebo controls compared with unirradiated). Intraperitoneal administration of ShK-170 (100 μg/kg) once daily, starting from the time of radiation and continued for 3 days, decreased radiation-induced loss of neurons in the cortex and hippocampus ($P < .05$; ShK-170–treated vs placebo control; Fig. 7A–D). NPCs (BrdU+/NeuN+ cells) are commonly found in the SGZ of the brain, where they proliferate, renew themselves, and differentiate into neurons. The number of BrdU+/NeuN+ cells in the SGZ in the dentate gyrus was evaluated at 14 days post-irradiation. The number of BrdU+/NeuN+ cells was reduced in irradiated placebo-control mice, indicative of diminished neurogenesis ($P < .05$; radiated placebo control vs unirradiated; Fig. 7E and F). ShK-170 (100 μg/kg once daily for 7 consecutive days starting from the time of radiation) enhanced the number of BrdU+/NeuN+ NPCs in the SGZ ($P < .05$; ShK-170–treated vs placebo control; Fig. 7E and F). These data suggest that ShK-170 enhances neurorestoration and attenuates brain injury induced by radiation.
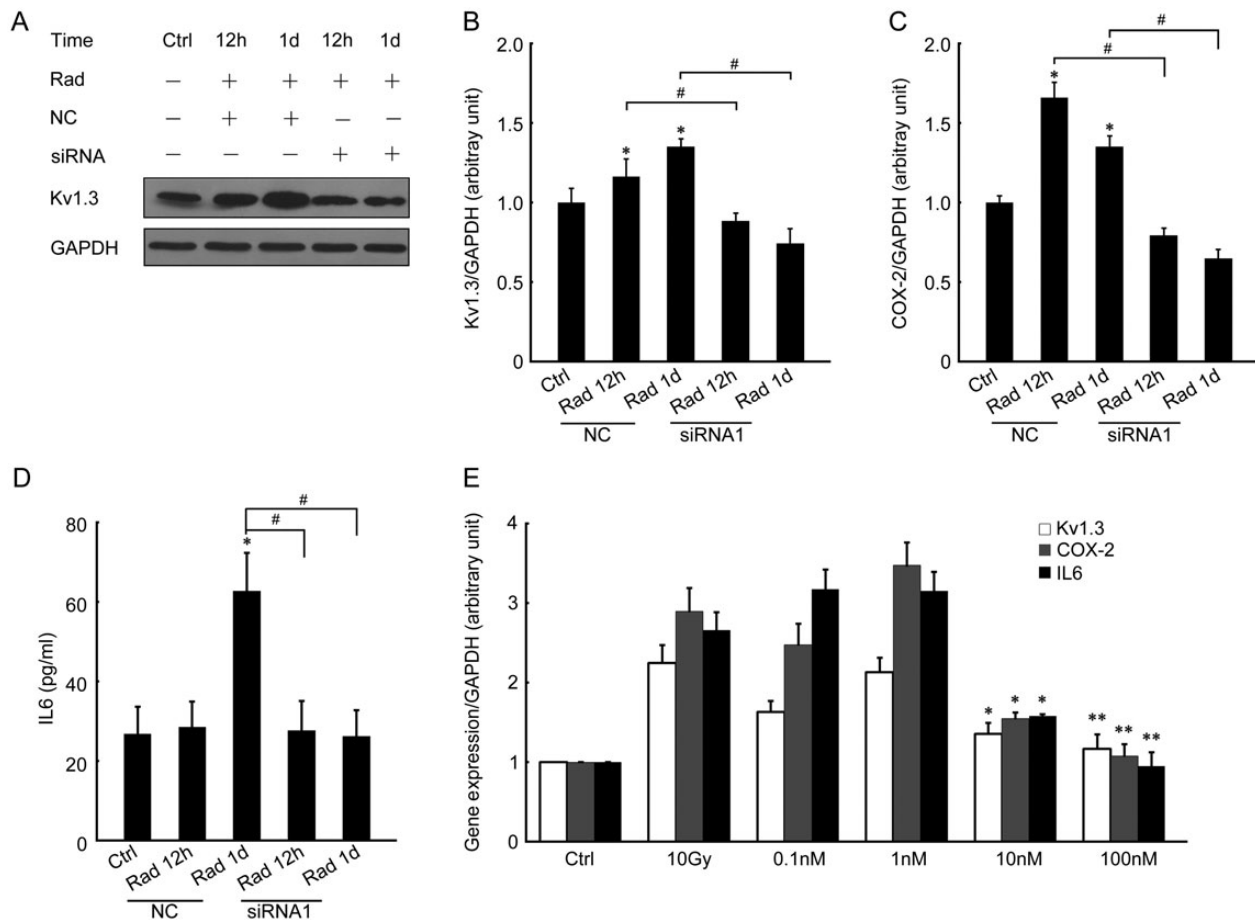
Fig. 5. Genetic silencing or pharmacological blockade of Kv1.3 prevents microglial activation. (A) Kv1.3-specific siRNA significantly inhibits Kv1.3 protein expression in transfected BV2 microglia. (B) Densitometric analysis of data in (A). Mean ± SEM; *$P < .05$ compared with unirradiated controls; #$P < .05$ when Kv1.3-specific siRNA-transfected radiated group vs radiated group; $n = 3$. (C, D) Kv1.3-specific siRNA suppresses radiation-induced increase in Cox-2 and IL-6. *$P < .05$ compared with unirradiated controls; #$P < .05$ when Kv1.3-specific siRNA-transfected irradiated group is compared with irradiated group; $n = 3$. (E) Densitometric scan showing that ShK-170 at 10 and 100 nM suppresses radiation-induced increases in Kv1.3, Cox-2, and IL-6 in microglia. *$P < .05$ compared with irradiated group; **$P < .01$ compared with irradiated group; $n = 3$.

Discussion

Radiation, a mainstay adjuvant therapy for cancers of the brain, head, and neck, carries the risk of neurologic injury including focal cerebral necrosis, neurocognitive deficits, cerebrovascular disease, myelopathy, and brachial plexopathy. Here we report that ShK-170, a selective inhibitor of the voltage-gated Kv1.3 potassium channel, significantly reduces radiation-induced brain injury in mice. In irradiated mice treated with placebo, MRI scans at week 16 following a 30-Gy radiation dose to the head caused significant enlargement of the lateral ventricles, indicative of cortical atrophy. In striking contrast, the volume of the lateral ventricles in mice that received 3 once-daily i.p. injections of ShK-170 immediately after radiation was similar to that of unirradiated mice. This therapeutic effect is due to suppression of microglial activation, prevention of activated microglia-mediated neurotoxicity, and promotion of neurogenesis. So far, there is no generally accepted animal model for irradiated brain injury. In the treatment of patients with head and neck or brain tumors, normally fractionated radiotherapy was used. Yet, in an animal model, it is difficult to

mimic this regimen, for animals cannot tolerate this high dose. Single radiation has been used more widely than fractionated radiation. In this study, single radiation was used to develop the animal model.

Brain irradiation was accompanied by microglial activation and production of proinflammatory factors corroborating previous reports,[40] and we detected a parallel increase in Kv1.3 mRNA and protein in microglia in brain-irradiated mice. The results suggested that Kv1.3 channel expression was regulated at the transcriptional level. The underlying signaling pathways that increase Kv1.3 channel expression after radiation remain unclear. Report 41 has shown that in HIV-1 infected brain, HIV-1 Tat protein induced Kv1.3 channel expression and consequent microglia activation through the signaling pathway of extracellular signal-regulated kinase (ERK)1/2 mitogen-activated protein kinase (MAPK). In the study, ERK1/2 phosphorylation was enhanced by Tat exposure. U0126 was used to inhibit MAP/ERK kinase MEK1 and MEK2, the MAPK kinases responsible for phosphorylation of ERK1/2 MAPK. Reduction of ERK1/2 MAPK activity using U0126 markedly decreased the expression levels of microglial Kv1.3.[41] Also
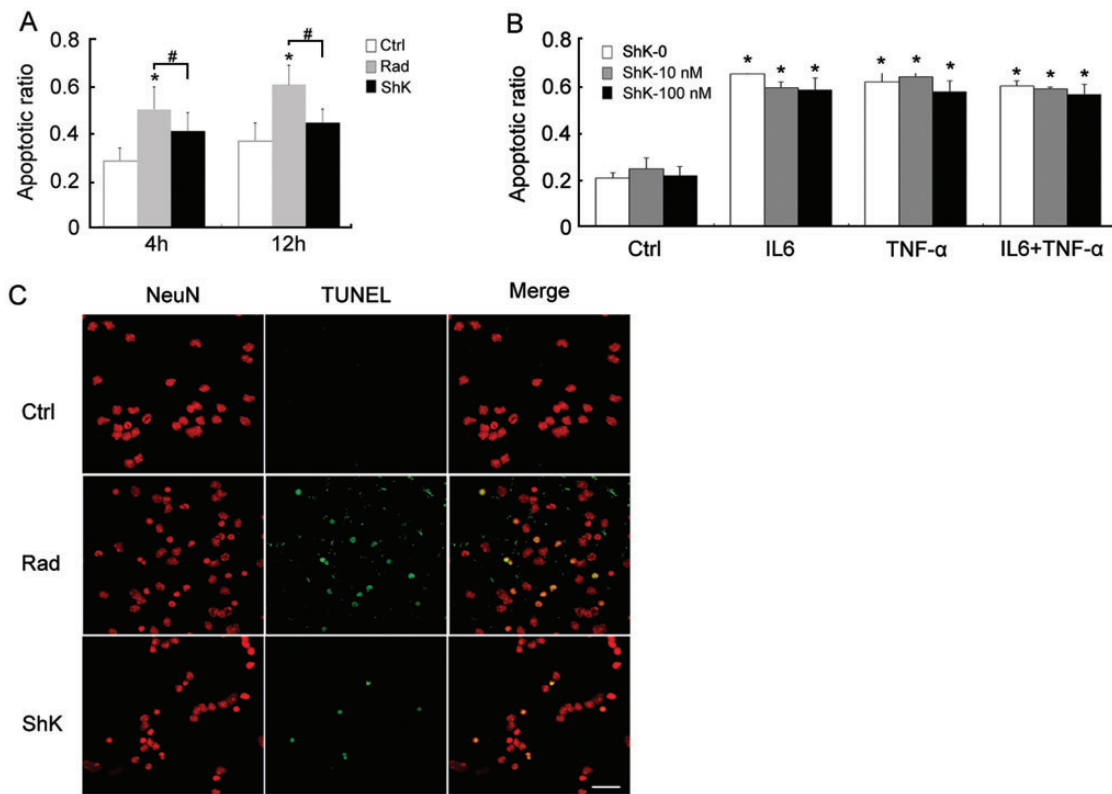
Fig. 6. ShK-170 prevents neurotoxicity by radiation-activated microglia. (A) Primary neurons were cocultured with microglia in a transwell system. Neurons were immunostained with NeuN, and apoptotic neurons were recognized through TUNEL staining. The ratio of apoptotic neurons to live neurons (apoptotic ratio) is shown. ShK-170 (100 nM) was effective in preventing radiation-mediated neurotoxicity; *$P = .0001$ at 4 h and $P = .033$ at 12 h when the apoptotic ratio of neurons cocultured with radiated microglia is compared with that of neurons cocultured with unirradiated control group; #$P < .01$ when the apoptotic ratio of neurons cocultured with irradiated microglia pretreated with ShK-170 is compared with that of neurons cocultured with irradiated microglia; $n = 3$. (B) Recombinant IL-6 and TNF-α induced apoptosis of neurons; mean $\pm$ SEM; *$P < .05$ when the apoptotic ratio of neurons untreated is compared with that of IL-6– or TNF-α–treated neurons. ShK-170 (100 nM) pretreatment did not prevent apoptosis in neurons exposed to recombinant IL-6 and TNF-α, indicating that its protective effect is due solely to its effect on microglia; $n = 3$. (C) Representative images of primary neurons (immunostained with anti-NeuN, red) cocultured with microglia to show the apoptotic neurons (stained with TUNEL, green). Scale bar, 50 μm.

phosphatidylinositol-3 kinase and p38 MAPK have been shown in literature to be involved in mediating Kv1.3 expression and microglial activation.[20] The exact signal transduction pathways that initiated Kv1.3 expression and microglial activation after radiation merit further investigation.

Genetic silencing with a Kv1.3-specific siRNA and pharmacological blockade with ShK-170 in radiated microglia both significantly reduced the production of proinflammatory factors. ShK-170 also effectively reduced microglial activation and production of proinflammatory factors in vivo following a single dose of radiation to the head. These results are consistent with the reported upregulation of Kv1.3 during microglial activation and the channel's involvement in the respiratory burst during microglial killing.[21] It is noted that the effect of Kv1.3 after radiation might also partly come from activation of this channel protein, in addition to the upregulation of expression of Kv1.3.

Although radiation can cause neuronal apoptosis directly, radiation-activated microglia can aggravate this injury through the production of proinflammatory factors such as IL-6, Cox-2, and TNF-α. Our study showed that ShK-170 significantly reduced radiation-activated microglia–mediated neurotoxicity but was ineffective at protecting neurons from the direct neurotoxic effects of recombinant IL-6 and TNF-α. ShK-170 therapy also reduced neuronal damage in the cortex and the CA3 region of the hippocampus, enhanced NPC proliferation, and suppressed microglia-mediated neurotoxicity. These results demonstrate that ShK-170 limits radiation-induced brain injury by targeting 2 key processes: suppression of microglia-mediated neuroinflammation, thereby protecting neurons from proinflammatory factor–mediated toxicity, and promotion of neurogenesis and neurorestoration.

Since radiation-induced brain injury is a severe complication of therapeutic irradiation for tumors affecting the head, neck, and brain, an imaging examination such as MRI, MR spectroscopy, PET-CT, or even brain biopsy is needed to prove that the brain injury is caused by radiation, not by brain metastasis of head and neck cancers or brain tumor recurrence. In addition, treatment of this complication should be started only after the primary tumor is controlled. If there is any chance of cancer metastasis or recurrence, cancer should always be treated with priority. In this scenario, blockade of Kv1.3 with ShK-170 in radiation-induced brain injury is safe.
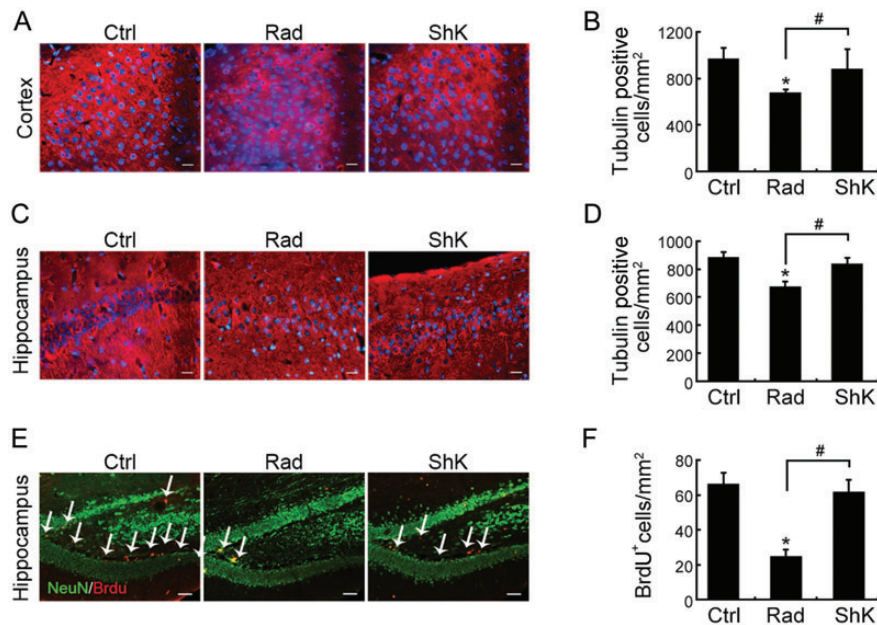
Fig. 7. ShK-170 prevents neurotoxicity by radiation-activated microglia. (A) Representative sections from cortex immunostained with anti–β-tubulin (red) and anti–4′,6′-diamidino-2-phenylindole (DAPI; blue). Scale bar, 20 μm. Data are from 2 independent experiments. (B) Quantification of viable neurons in layer-3 cortex, *$P < .01$ when irradiated group is compared with unirradiated control group; #$P < .05$ when ShK-170–treated group is compared with irradiated group; $n = 5$. (C) Representative sections from hippocampus immunostained with anti–β-tubulin (red) and anti-DAPI (blue). Scale bar, 20 μm. (D) Quantification of viable neurons in CA3 hippocampus. *$P < .01$ when irradiated group is compared with unirradiated control group; #$P < .05$ when ShK-170–treated group is compared with irradiated group; $n = 5$. (E) Representative sections from hippocampus immunostained with anti-NeuN (green) and anti-BrdU (red). Scale bar, 50 μm. Groups same as for (A) except that the treatment period for ShK-170 is 7 consecutive days and the animals were sacrificed at 14 days after irradiation ($n = 6$ in each group). (F) Quantitative analysis showed decreased numbers of BrdU$^+$/NeuN$^+$ NPCs 14 days after irradiation and restoration with ShK-170. *$P < .01$ when irradiated group is compared with unirradiated control group; #$P < .05$ when ShK-170–treated group is compared with irradiated group; $n = 6$.

A stabilized analog of ShK-170, ShK-186, has completed preclinical pharmacokinetic and toxicity studies and is being evaluated in first-in-human phase 1 clinical trials.[26,38,42–47] ShK-186 and clofazimine,[48] therapies for leprosy with Kv1.3-blocking activity, merit evaluation for their ability to limit neurologic injury following therapeutic radiation for brain, head, and neck cancers. Kv1.3 blockers may have an advantage over corticosteroids, which are effective inhibitors of neuroinflammation and brain edema following therapeutic radiation but have the disadvantage of inhibiting neurogenesis. It remains to be seen whether Kv1.3 blockers exhibit any advantage over other agents such as indomethacin and minocycline, which both inhibit microglial activation and are neuroprotective.[31,33,34]

Supplementary Material

Supplementary material is available online at *Neuro-Oncology* (http://neuro-oncology.oxfordjournals.org/).

Conflict of interest statement. K. George Chandy is an inventor of a patent on ShK-170 and ShK-186 that has been licensed by the University of California to Kineta Inc., Seattle, WA. In the past, he served as a consultant to Kineta to help with preclinical development of ShK-186. None of the other authors have any conflict of interest.

References

1. Bondy ML, Scheurer ME, Malmer B, et al. Brain tumor epidemiology: consensus from the Brain Tumor Epidemiology Consortium. *Cancer*. 2008;113:1953–1968.

2. Howlader N, Noone AM, Krapcho M, et al. SEER cancer statistics review, 1975–2009 (vintage 2009 populations). Bethesda, MD: National

Cancer Institute; 2011. http://seer.cancer.gov/csr/1975_2009_pops09. Accessed November 10, 2013.

3. Jemal A, Bray F, Center MM, Ferlay J, Ward E, Forman D. Global cancer statistics. *CA Cancer J Clin*. 2011;61:69–90.

4. Dropcho EJ. Neurotoxicity of radiation therapy. *Neurol Clin*. 2010;28: 217–234.

5. Crossen JR, Garwood D, Glatstein E, Neuwelt EA. Neurobehavioral sequelae of cranial irradiation in adults: a review of radiation-induced encephalopathy. *J Clin Oncol*. 1994;12:627–642.

6. Giglio P, Gilbert MR. Neurologic complications of cancer and its treatment. *Curr Oncol Rep*. 2010;12:50–59.

7. Ramanan S, Kooshki M, Zhao W, Hsu FC, Robbins ME. PPARalpha ligands inhibit radiation-induced microglial inflammatory responses by negatively regulating NF-kappaB and AP-1 pathways. *Free Radic Biol Med*. 2008;45:1695–1704.

8. Monje ML, Vogel H, Masek M, Ligon KL, Fisher PG, Palmer TD. Impaired human hippocampal neurogenesis after treatment for central nervous system malignancies. *Ann Neurol*. 2007;62:515–520.

9. Hwang SY, Jung JS, Kim TH, et al. Ionizing radiation induces astrocyte gliosis through microglia activation. *Neurobiol Dis*. 2006;21: 457–467.

10. Ekdahl CT, Claasen J, Bonde S, Kokaia Z, Lindvall O. Inflammation is detrimental for neurogenesis in adult brain. *Proc Natl Acad Sci U S A*. 2003;100:13632–13637.

11. Monje ML, Palmer T. Radiation injury and neurogenesis. *Curr Opin Neurol*. 2003;16:129–134.

12. Block ML, Hong JS. Microglia and inflammation-mediated neuro-degeneration: multiple triggers with a common mechanism. *Prog Neurobiol*. 2005;76:77–98.

13. Kempermann G, Neumann H. Neuroscience. Microglia: the enemy within? *Science*. 2003;302:1689–1690.

14. Kyrkanides S, Moore AH, Olschowka JA, et al. Cyclooxygenase-2 modulates brain inflammation-related gene expression in central nervous system radiation injury. *Brain Res Mol Brain Res*. 2002;104: 159–169.

15. Raju U, Gumin GJ, Tofilon PJ. NF kappa B activity and target gene expression in the rat brain after one and two exposures to ionizing radiation. *Radiat Oncol Investig*. 1999;7:145–152.

16. Achanta P, Fuss M Jr, Martinez JL. Ionizing radiation impairs the formation of trace fear memories and reduces hippocampal neurogenesis. *Behav Neurosci*. 2009;123:1036–1045.

17. Mizumatsu S, Monje ML, Morhardt DR, Rola R, Palmer TD, Fike JR. Extreme sensitivity of adult neurogenesis to low doses of X-irradiation. *Cancer Res*. 2003;63:4021–4027.

18. Acharya MM, Christie LA, Lan ML, et al. Rescue of radiation-induced cognitive impairment through cranial transplantation of human embryonic stem cells. *Proc Natl Acad Sci U S A*. 2009;106: 19150–19155.

19. Menteyne A, Levavasseur F, Audinat E, Avignone E. Predominant functional expression of Kv1.3 by activated microglia of the hippocampus after status epilepticus. *PLoS One*. 2009;4:e6770.

20. Khanna R, Roy L, Zhu X, Schlichter LC. K+ channels and the microglial respiratory burst. *Am J Physiol Cell Physiol*. 2001;280:C796–C806.

21. Fordyce CB, Jagasia R, Zhu X, Schlichter LC. Microglia Kv1.3 channels contribute to their ability to kill neurons. *J Neurosci*. 2005;25: 7139–7149.

22. Cahalan MD, Chandy KG. The functional network of ion channels in T lymphocytes. *Immunol Rev*. 2009;231:59–87.

23. Mullen KM, Rozycka M, Rus H, et al. Potassium channels Kv1.3 and Kv1.5 are expressed on blood-derived dendritic cells in the central nervous system. *Ann Neurol*. 2006;60:118–127.

24. Liebau S, Propper C, Bockers T, et al. Selective blockage of Kv1.3 and Kv3.1 channels increases neural progenitor cell proliferation. *J Neurochem*. 2006;99:426–437.

25. Wang T, Lee MH, Johnson T, et al. Activated T-cells inhibit neurogenesis by releasing granzyme B: rescue by Kv1.3 blockers. *J Neurosci*. 2010;30: 5020–5027.

26. Beeton C, Pennington MW, Wulff H, et al. Targeting effector memory T cells with a selective peptide inhibitor of Kv1.3 channels for therapy of autoimmune diseases. *Mol Pharmacol*. 2005;67:1369–1381.

27. Maezawa I, Zimin PI, Wulff H, Jin LW. Amyloid-beta protein oligomer at low nanomolar concentrations activates microglia and induces microglial neurotoxicity. *J Biol Chem*. 2011;286:3693–3706.

28. Rojanathammanee L, Murphy EJ, Combs CK. Expression of mutant alpha-synuclein modulates microglial phenotype in vitro. *J Neuroinflammation*. 2011;8:44.

29. Rosi S, Andres-Mach M, Fishman KM, Levy W, Ferguson RA, Fike JR. Cranial irradiation alters the behaviorally induced immediate-early gene arc (activity-regulated cytoskeleton-associated protein). *Cancer Res*. 2008;68:9763–9770.

30. Wojtowicz JM, Kee N. BrdU assay for neurogenesis in rodents. *Nat Protoc*. 2006;1:1399–1405.

31. Mandell JG, Neuberger T, Drapaca CS, Webb AG, Schiff SJ. The dynamics of brain and cerebrospinal fluid growth in normal versus hydrocephalic mice. *J Neurosurg Pediatr*. 2010;6:1–10.

32. Chen CC, Tung YY, Chang C. A lifespan MRI evaluation of ventricular enlargement in normal aging mice. *Neurobiol Aging*. 2011;32: 2299–2307.

33. Morris R. Developments of a water-maze procedure for studying spatial learning in the rat. *J Neurosci Methods*. 1984;11:47–60.

34. Wang Z, Yang D, Zhang X, et al. Hypoxia-induced down-regulation of neprilysin by histone modification in mouse primary cortical and hippocampal neurons. *PLoS One*. 2011;6:e19229.

35. Panagiotakos G, Alshamy G, Chan B, et al. Long-term impact of radiation on the stem cell and oligodendrocyte precursors in the brain. *PLoS One*. 2007;2:e588.

36. Olschowka JA, Kyrkanides S, Harvey BK, et al. ICAM-1 induction in the mouse CNS following irradiation. *Brain Behav Immun*. 1997;11: 273–285.

37. Li YQ, Chen P, Haimovitz-Friedman A, Reilly RM, Wong CS. Endothelial apoptosis initiates acute blood-brain barrier disruption after ionizing radiation. *Cancer Res*. 2003;63:5950–5956.

38. Beeton C, Wulff H, Standifer NE, et al. Kv1.3 channels are a therapeutic target for T cell–mediated autoimmune diseases. *Proc Natl Acad Sci U S A*. 2006;103:17414–17419.

39. Arvidsson A, Collin T, Kirik D, Kokaia Z, Lindvall O. Neuronal replacement from endogenous precursors in the adult brain after stroke. *Nat Med*. 2002;8:963–970.

40. Monje ML, Toda H, Palmer TD. Inflammatory blockade restores adult hippocampal neurogenesis. *Science*. 2003;302:1760–1765.

41. Liu J, Xu P, Collins C, et al. HIV-1 Tat protein increases microglial outward K(+) current and resultant neurotoxic activity. *PLoS One*. 2013;8: e64904.

42. Pennington MW, Beeton C, Galea CA, et al. Engineering a stable and selective peptide blocker of the Kv1.3 channel in T lymphocytes. *Mol Pharmacol*. 2009;75:762–773.

43. Chi V, Pennington MW, Norton RS, et al. Development of a sea anemone toxin as an immunomodulator for therapy of autoimmune diseases. *Toxicon*. 2012;59:529–546.

44. Gilhar A, Bergman R, Assay B, Ullmann Y, Etzioni A. The beneficial effect of blocking Kv1.3 in the psoriasiform SCID mouse model. *J Invest Dermatol*. 2011;131:118–124.

45. Hao B, Chen ZW, Zhou XJ, et al. Identification of phase-I metabolites and chronic toxicity study of the Kv1.3 blocker PAP-1 (5-(4-phenoxybutoxy)psoralen) in the rat. *Xenobiotica*. 2011;41:198–211.

46. Matheu MP, Beeton C, Garcia A, et al. Imaging of effector memory T cells during a delayed-type hypersensitivity reaction and suppression by Kv1.3 channel block. *Immunity*. 2008;29:602–614.

47. Pereir LE, Villinger F, Wulff H, Sankaranarayanan A, Raman G, Ansari AA. Pharmacokinetics, toxicity, and functional studies of the selective Kv1.3 channel blocker 5-(4-phenoxybutoxy)psoralen in rhesus macaques. *Exp Biol Med (Maywood)*. 2007;232:1338–1354.

48. Ren YR, Pan F, Parvez S, et al. Clofazimine inhibits human Kv1.3 potassium channel by perturbing calcium oscillation in T lymphocytes. *PLoS One*. 2008;3:e4009.